Visualization and quantitative analysis of spatiotemporal behavior in a first-order thermal spin transition: A stress-driven multiscale process

A. Slimani,[1] F. Varret,[1] K. Boukheddaden,[1,*] C. Chong,[1] H. Mishra,[1] J. Haasnoot,[2] and S. Pillet[3]

[1]*Groupe d'Etudes de la Matière Condensée, CNRS-Université UMR 8635, Universite de Versailles, 45 Avenue des Etats Unis, 78035 Versailles, France*

[2]*Leiden Institute of Chemistry, Gorlaeus Laboratories, Leiden University, P.O. Box 9502, 2300 RA Leiden, The Netherlands*

[3]*Laboratoire de Cristallographie, Résonance Magnétique et Modélisations, UMR CNRS 7036, Institut Jean Barriol, Nancy-Université, BP239, 54506 Vandoeuvre les Nancy, France*

(Received 10 May 2011; revised manuscript received 25 July 2011; published 26 September 2011)

We investigated by optical microscopy the propagation of the thermal spin transition in $[Fe(btr)_2(NCS)_2]\cdot H_2O$·(btr = bis-triazole) single crystals. Using high-quality fresh crystals embedded in oil we could follow the transformation front of the on-cooling transition. We observed in detail a linear front propagating through the entire crystal at extremely slow velocity, ∼2.5 μm/s on average. The analysis of the temporal dependences of the optical densities (OD) at given positions within a Kolmogorov-Johnson-Mehl-Avrami (KJMA) law led to an exponent ∼0.6, typical for a process governed by planar diffusion. It is inferred that the spin transition is a multiscale process. The agreement with a previous structural investigation, analyzed in terms of an average KJMA law, is shown. We conclude that the stresses generated by the volume change associated with the spin transformation are the driving force for the propagation of the nucleation and growth mechanism. The role of defects is discussed and optical effects specific of the experiment are evidenced.

DOI: 10.1103/PhysRevB.84.094442 PACS number(s): 75.30.Wx, 64.60.Q−, 64.70.K−, 07.60.Pb

I. INTRODUCTION

Spin transition solids are archetype compounds of switchable molecular solids (SMS), that is, they may exhibit a neat first-order transition between low-temperature low-spin (LS) and high-temperature high-spin (HS) states with well-characterized hysteresis. The switching between spin states can be triggered by several means such as temperature and pressure variations, irradiation in the visible range, pulsed magnetic field, and ligand photo-isomerisation. It can be monitored by various techniques because of the large changes in the physical properties (structure, volume, color, magnetization, dielectric moment, specific heat, etc.) and spectroscopic properties (optical, Raman, Mössbauer, etc.) under the effect of the spin-state change at the molecular and lattice levels. General information can be found in a recent book.[1] In brief, the thermal spin transition is driven by the entropy difference between the LS and HS states: HS has a higher electronic degeneracy and larger density of vibrational states.[2,3] The occurrence of first-order transition with hysteresis is assigned to the presence of elastic interactions between the spin-crossover molecular units.[4,5] The experimental features of the thermal transition are most usually obtained by magnetic or optical techniques that statistically measure the HS fraction, n_{HS}, which is the usual order parameter of the system. Most of the literature work on spin transitions was acquired from polycrystalline samples, and for the thermal transition it was almost exclusively restricted to the characterization of the quasistatic hysteresis of the system. Only recently studies aiming to determine the transition kinetics were performed on high-quality single crystals by x-ray diffraction[6] on the present compound $[Fe(btr)_2(NCS)_2]\cdot H_2O$ (btr = bis-triazole), here denoted Fe-btr, and by optical absorption spectroscopy[7] on the compound $[Fe(bbtr)_3](ClO_4)_2$ (bbtr = 1,4-di(1,2,3-triazol-1-yl)butane), denoted Fe-bbtr. These works accurately characterized the behavior of an individual single crystal, but only in average, and we intend here to go a step further and analyze the propagation of the transition through the crystal by using optical microscopy. Indeed it was pointed out by Mnyukh since the 1970s that optical microscopy was a crucial tool for elucidating the nucleation and growth character of solid-state transitions.[8] We quote here a few striking examples of application of optical microscopy selected from a recent review[9] dealing with organic crystals,[10–13] dielectrics,[14] or liquid-crystals.[15] Also, optical microscopy was recently introduced in the field of spin-transition solids through a few qualitative investigations, which evidenced the propagation of more or less well-defined transformation fronts.[16–20] We present here a quantitative investigation based on high-quality single crystals of Fe-btr, which provide the data needed for a first description of the propagation process of a spin transition in physical terms.

The development of optical microscopy for investigating the properties of SMS is quite recent. After a pioneering work at Bern,[21] which unfortunately was not followed, the method really started on the example of the photo-induced transformation of the well-known spin-transition compound $[Fe(ptz)_6](BF_4)_2$ (ptz = 1-n-propyltetrazole), denoted Fe-ptz.[21] Optical microscopy revealed to be useful for elucidating the mysterious "two-step" character of the relaxation curve of Fe-bbtr at the vicinity of the transition temperature.[19] The latter work allowed us to evidence the crucial impact of stresses generated by the volume change associated with the electronic transformation. Stresses were capable of shifting by more than 20 K the on-cooling transition temperature of the constrained part of the crystal. In addition stresses created irreversible damage of the crystals due to the brittleness of these molecular solids. Consequently the observation of neat transformation fronts (that is, HS/LS interfaces) appears to be restricted to

the case of fresh crystals undergoing their first transition. We also showed that optical microscopy could be used as a colorimetric approach for separating the electronic and structural transformations involved in the thermal transition of Fe-ptz.[23]

We now briefly summarize the results of our previous investigation of the Fe-btr compound.[20] This system was selected because of the large optical absorbance of the crystal in the LS state.[24] The available material consisted in lower-quality crystals selected from a batch prepared at Leiden (author J.H.) for previous investigations of polycrystalline samples.[25,26] We observed the presence of well-defined transformation fronts, but their propagation was far from regular due to the presence of macroscopic defects. The propagation of the on-cooling transition of fresh crystals could be completed in isothermal conditions, but the subsequent on-heating transition was no more homogenous and it was spread over a large temperature interval due to the damage undergone by the previous on-cooling transformation. We also observed a couple of high-quality crystals left from the previous structural investigation. The first one did not show a well-defined front, and this was assigned to the crystal thickness (which does not favor the minimization of the interface area); the second one showed multiple nucleation sites which were not suited for a first quantitative approach. On the basis of these promising results further high-quality crystals were grown by the crystallography group (author S.P.) for the more detailed investigation, which is reported here.

The basic properties of Fe-btr were reported in Ref. 27. Previous diffraction investigation on high-quality Fe-btr single crystals provided features typical for a nucleation and growth process both in the thermal transition[6] and the photo-induced transition regime, which actually was investigated sooner.[28] The structure of Fe-btr[27] was described as a stacking along the crystallographic a axis of 2D layers connected by van der Waals interactions and weak hydrogen bonds through a lattice water molecule. Each layer consists of an almost regular square lattice of Fe(II) cations bridged by bidentate btr ligands, leading to a highly cooperative polymeric 2D lattice.

The crystals under investigation had typical size, $\sim 500 \times 200 \times 100$ μm. These crystals were embedded in silicon oil for protection against dehydration and located in an exchange-gas cell previously described;[23] the rest of the experimental device was also previously described.[22] During the transformation stages of the crystal we automatically recorded the computer (PC) screen by using the CamStudio software and simultaneously recorded snapshots every $\sim$1.5 sec on average. The working assumption here, following Ref. 22, is that the optical-density data (OD $= \log_{10}(I_0/I)$), I_0 = bright field intensity, I = transmitted intensity) merely scale to the spin fraction (e.g., the HS fraction n_{HS}).

A set of typical images is shown in Fig. 1 for a selected crystal (labeled A) sitting with the crystallographic axis a of the monoclinic structure, approximately parallel to the microscope axis. At room temperature all fresh crystals when observed between crossed polarizers showed beautiful extinctions with neutral lines parallel to the quasiperpendicular edges of the natural face, which were assigned to the b and c crystallographic axes of the structure. On cooling, the oil film underwent a glassy transition liquid around 200 K and usually cracked a few degrees before the occurrence of the spin transition. Transformation of crystal A, at cooling rate 0.2 K/min, started from a corner of the crystal at 102.6 K with a grossly circular shape, and after a while it formed a well-defined linear front, which propagated through the crystal at a rather constant velocity $\sim$2.3 μm/s, as will be determined

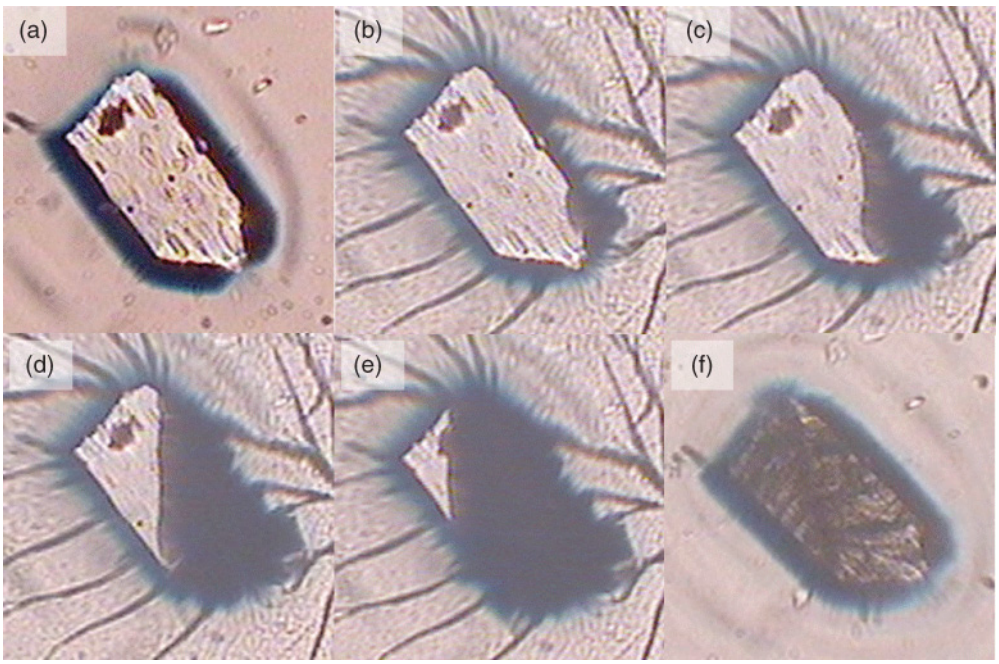

FIG. 1. (Color online) Selected images of a fresh Fe-btr crystal A embedded in oil (a) at room temperature, (b)–(e) under cooling at 0.2 K/min, and (f) after complete thermal cycle. Respective temperatures are 295, 102.67, 102.55, 102.50, 101.43, and 260 K. Image size 450×450 μm. A video was made with the full set of images, see Supplemental Material.[29]

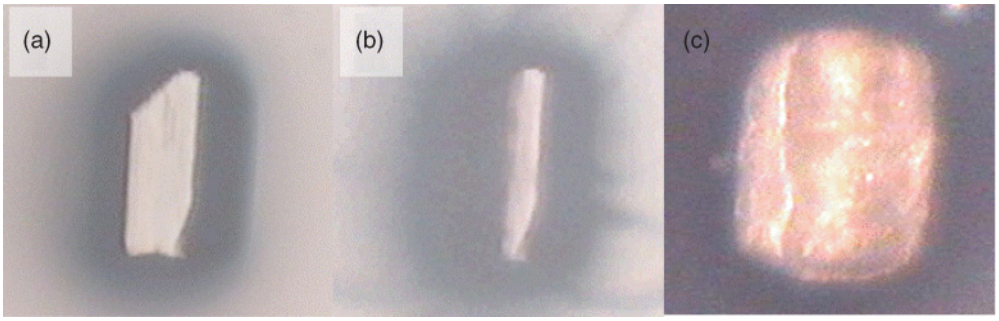

FIG. 2. (Color online) Selected images of a fresh Fe-btr crystal B embedded in oil (a) at room temperature, (b) under cooling at 0.05 K/min, and (c) after complete thermal cycle. Respective temperatures are 295, 99, and 260 K. Image size 450 × 450 μm. A video set was realized for the cooling process, see Supplemental Material.[30]

in the following. The transformation was completed within ∼100 s. The contrasted character of the images shows that the HS/LS interface (∼planar transformation front) is roughly parallel to the microscope axis (structural axis *a*). Such an orientation obviously minimizes the elastic energy for crystals in the shape of platelets and also corresponds to propagation predominantly within the structural 2D layers. This orientation is consistent with the preliminary investigation of thinner crystals and such energy considerations might explain the absence of a well-defined front in the thicker crystal previously reported.

We show in Fig. 2 the on-cooling transition of a thicker crystal, denoted B. Thickness ∼170 μm was determined by focusing the image on top and aside the crystal, successively. At cooling rate 0.05 K/min, the transformation started at 99 K and occurred in two steps: quasi-immediately, half of the crystal turned to the LS state, and afterward the transformation of the second half proceeded smoothly with a more diffuse front that was roughly parallel to the long edges of the crystal (see video B). Transformation of crystal B was completed within only ∼14 s with a propagation velocity ∼10 μm/s. These features show that the actual temperature of the transformation and the presence of internal stresses have large impacts on the propagation. The temperature effect is easily understood in terms of over-cooling with respect to the (equilibrium) transition temperature: the larger the over-cooling, the faster the relaxation to the stable state. The observed impact of the cooling rate—the smaller the cooling rate, the larger the overcooling—has to be confirmed by further systematic investigations. (Such investigation will require a statistical approach based on the first cooling of fresh crystals.) Assuming that this impact is confirmed, we suggest that the stresses generated by the thermal gradients (the larger the scan rate, the larger the thermal gradients) may generate the nucleation centers needed for the transition. After rewarming crystal B was opalescent and displayed an amazing inhomogeneous expansion, which evidenced the onset of plastic deformations. To summarize, these qualitative observations suggest that the impact of the mechanical stresses on the propagation process of the spin transition may be extremely complex. The actual geometric and kinetic properties of the front may depend very sensitively on the shape of the sample and on the thermal temperature gradients associated with the heat flows generated by the temperature control. Also, it should be kept in mind that the transition generates intrinsic heat flows due to the entropy change.

The low-to-high spin transition (on heating) always took place in a very inhomogeneous way that we assign to the presence of inhomogeneous stresses generated during the previous on-cooling transition. In addition after thermal cycling, see Fig. 1(f), we always observed a large number of cracks on the crystals, a lower transmittance in bright field geometry, and a poorer extinction with reduced angular dependence for observations between crossed polarizers. The irreversible damage of the crystals presumably combines dislocations and fractures and was illustrated by the subsequent behavior of the crystals upon further cooling, which was basically different. For instance crystal A at the same cooling rate (0.2 K/min) displayed complex patterns with various orientations of the transformation front; the transition temperature was then ∼10 K higher, and the propagation velocity of the transformation front was reduced by a factor ∼2. In the following we shall focus on the data reported in Fig. 1, which seem to be close to ideal propagation behavior, that is, transformation with almost linear front, constant in orientation.

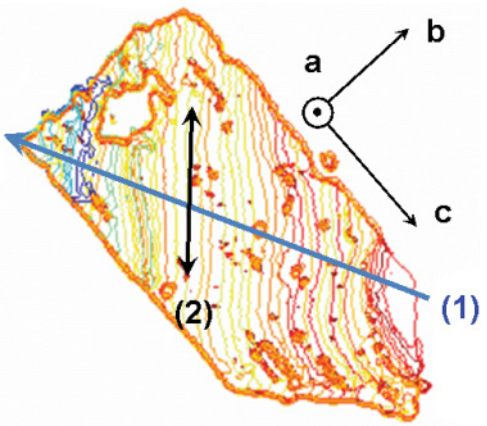

FIG. 3. (Color online) Contour lines of the LS area determined from the successive snapshots of crystal A, recorded every ∼1.5 sec. (1) is the reference line selected for determining the velocity of the transformation front. (2) is a segment parallel to the propagation front, selected for an accurate measurement of the local kinetics of the transformation.

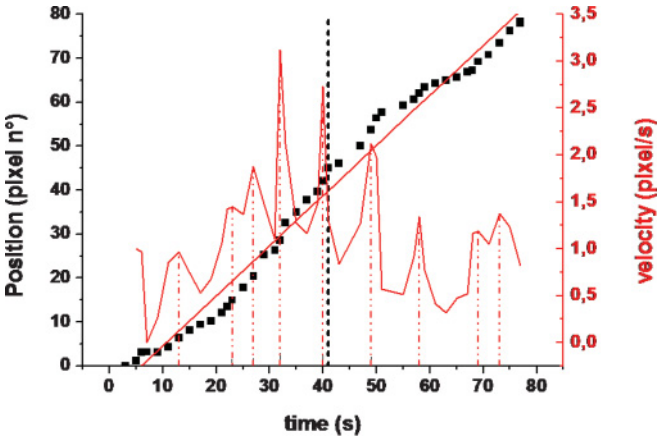

FIG. 4. (Color online) Plot of the crossing points between contour lines and reference line (1) of Fig. 3 vs time for determining the propagation velocity of the transformation front. The average slope 1.14 pixel/s = 1.14 × 2.25 ∼ 2.6 μm/s is obtained (2.3 μm/s once projected along the perpendicular to the transformation front). The dotted line refers to the position of segment (2) in the previous figure. The red curve describes the evolution of instantaneous velocity versus time.

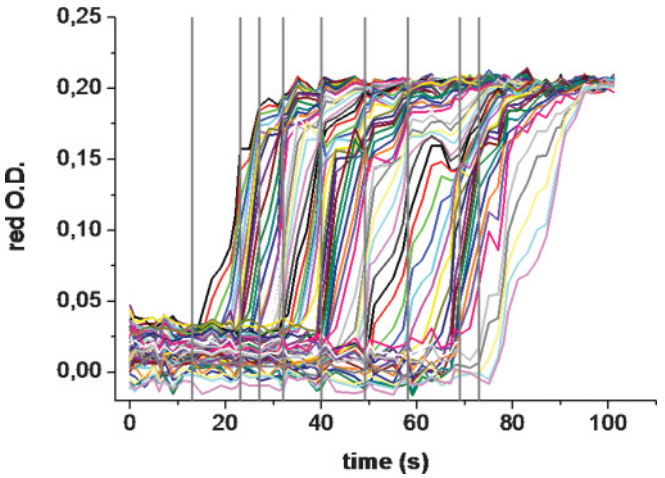

FIG. 5. (Color online) The time dependence of the red OD recorded at fixed positions along the reference line (1) during the propagation of the transition. The vertical lines represent the location of the velocity peaks of Fig. 4 and obviously overlap the Moiré fringes of the present plot.

A. Propagation of the transformation fronts

We report in Fig. 3 the successive positions of the propagation front through the fresh crystal A. For each microscope image we determined a "contour" line associated with a reference value in-between those of the LS and HS states. For instance the average value of the HS–LS OD, that is the geometric average of the HS–LS transmitted intensities, approximately corresponds to the spin fraction $n_{HS} = 1/2$. The transformation started from a corner and first proceeded with a rather circular front, reminiscent of a shock wave. Afterward the front progressively straightened and finally crossed the entire crystal with a rather stable orientation. From the successive positions of the front along a given "reference" line (1), shown in Fig. 3, an average propagation velocity could be determined, see Fig. 4. The instantaneous velocity derived from the plot of Fig. 4 exhibits sizable fluctuations. Similar features were found at the same times along other lines parallel to the reference line (1).

The rather constant character of the velocity along the transformation process—save for the presence of large fluctuations—has to be discussed. The process might be analyzed on the basis of the dynamics of twin boundaries in ferroelastic and ferroelectric materials when external force fields are applied.[31] Newton's law would require that the motion of interfaces under stress (that is the present case) or electric fields (in case of ferroelectric materials) has to be accelerated in the early stage of the propagation following a creep, depinning, and then a flow regime. These stages are hardly seen in the present experiments. At longer times, in the asymptotic regime, the interface propagates at a constant velocity that results from the solution of the dynamic equation of an over-damped system with no effective mass. We may speculate that the physical reason for this behavior is related to the dissipation of energy during the interfacial motion, either via phonons or via defects where acceleration over small distances (which here reaches ∼5 μm/s at maximum value) is stopped (minimum value 0.4 μm/s) by the presence of defects (or pinning sites). This accelerated/decelerated mechanism (which does not necessarily exist at the atomic level in case of extrinsic defects) leads to over-damp macroscopically the smooth propagation of the interface. Consequently the spurious aspect of the front velocity suggests that the propagation of the interface proceeds in the avalanche way. We also noticed the progressive transformation of the circular front in the early stages into a linear front as soon as the transition proceeds between parallel edges. The shape and the propagation velocity of the transformation front obviously depend on the limiting conditions. Further experiments are needed to document this point through more detailed experiments taking advantage of increased spatial and temporal resolutions, which in principle are possible.

We now turn to kinetic curves recorded at fixed positions along line (1), see Fig. 5. This set of curves could be used for monitoring the propagation of the transformation front, as well as the contour curves previously used, and it provided identical results. Figure 5 displays spectacular Moiré fringes that reveal stages of rapid increase of the LS fraction in groups of neighboring pixels, which are in the course of the transformation. These rapid stages of local transformation are correlated to the rapid stages of propagation of Fig. 4, which have been indicated by vertical lines on both figures. We also tried to correlate the fluctuations of the interface width, derived form the mid-position slope of each OD profile curve along line (1) to the velocity fluctuations. We built up correlation plots (width vs velocity), not shown here, which exhibited neither a clear relationship between the width and velocity fluctuations over the entire process nor purely random features associated with independent variables. They rather suggest a succession of propagation regimes over short periods of time, typically a few seconds, which compare to the average interval of time between the velocity peaks of Fig. 4. The system might switch between several propagation regimes during the course of the transition. This bold statement of course remains to

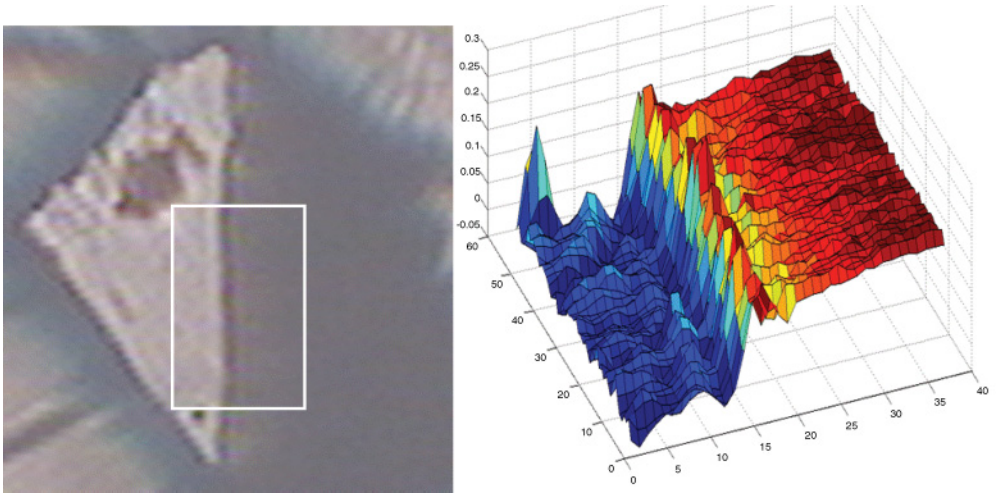

FIG. 6. (Color online) Pseudo-3D plot of the red OD data (right) inside the rectangular frame shown in the left image. The video of the complete process is included in Supplemental Material.[32]

be confirmed by further experiments but outlines an exciting frame for future investigations.

Figure 5 also shows interesting properties of the OD signal. The background value associated with the HS state (lower part of the curves) shows fluctuations associated with the presence of defects in the crystal. These defects are better detected on spatial plots such as those of Figs. 6 and 7. It may be noticed that the amplitude of the said fluctuations is sizably reduced in the LS state of the system. We think that this is a purely optical effect resulting from an irreversible increase of light scattering due to the creation of defects, as evidenced since our previous works on Fe(ptz) crystals.[22,23] Another intriguing feature of Figs. 6 and 7 is the presence of oscillations on each side of the LS/HS interface. These oscillations are also interpreted in optical terms, as due to variations of the refractive index of the crystal at the vicinity of the HS/LS interface, and reveal the presence of mechanical stresses. Such stresses are responsible for the deflection of the light beam and generate the shade of the interface as well as mirages on both sides of the interface, which are respectively seen as a ridge and valleys on the pseudo-3D plot of Fig. 6. These features appear on the images as dark and bright lines parallel to the front. In both cases (raw image or pseudo-3D plot) these lines are strongly disturbed by the occurrence of fluctuations, and we recommend watching the videos for taking advantage of the eye capability of treating noisy signals. Image processing of the spatiotemporal effects is planned and hopefully will be described in a future report.

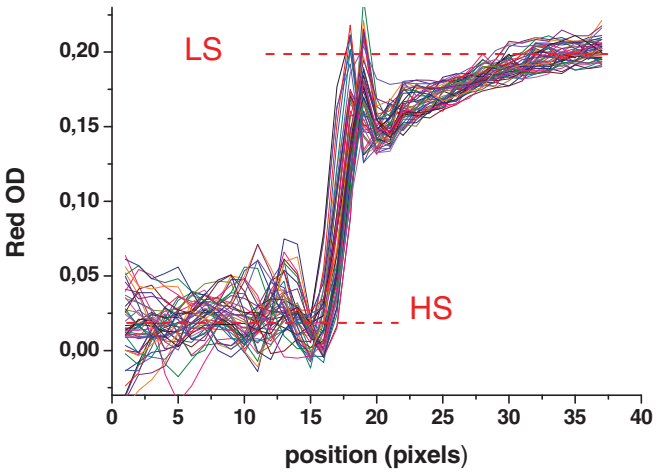

FIG. 7. (Color online) Profiles of red OD data from Fig. 1(d) along horizontal lines in the rectangular frame previously defined. Notice the oscillations of the optical signal on both side of the interface.

B. Local kinetics of the transformation

The local kinetics of the transformation is obtained, in principle, by monitoring the temporal evolution of the OD at given positions. However, the signal provided by a single pixel was rather noisy, and a statistical investigation was needed. For this we selected a set of pixels along segment (2) which could

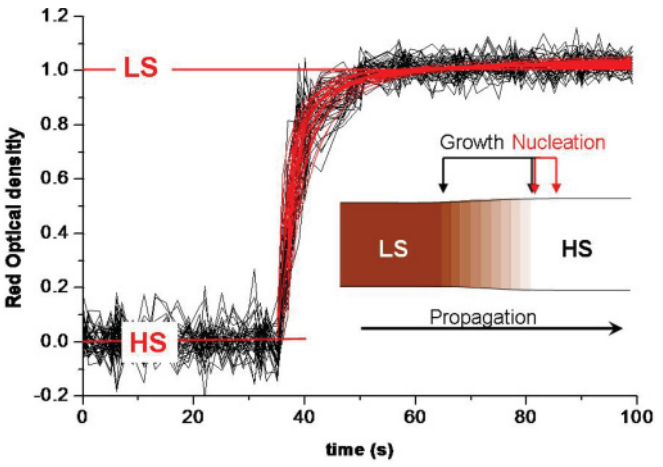

FIG. 8. (Color online) Red OD data reported for separate pixels along segment (2) of Fig. 3, which express the local kinetics of the HS→ LS transformation of crystal A. Black (red) lines stand for experimental data (fitted curves). Inset: a schematic view of the proposed propagation mechanism for the stress-driven nucleation and growth process.

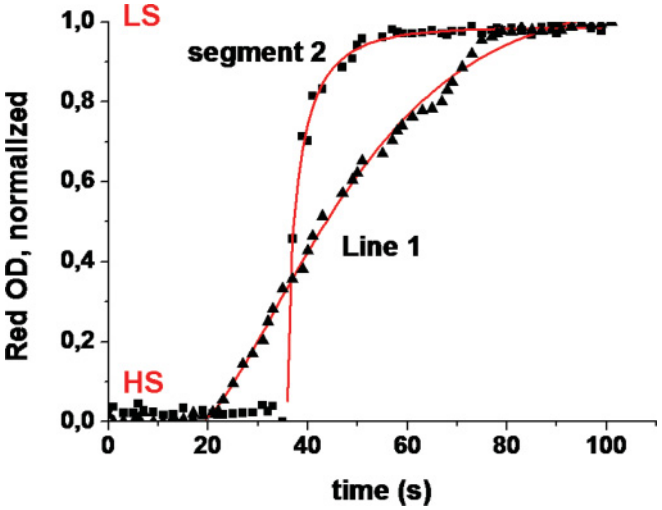

FIG. 9. (Color online) Average kinetic curves obtained by summation along line (1) or segment (2) with the best-fitted curves using Eq. (1).

transiently match at best the propagation front (at time $t =$ 41 s, precisely). Therefore the spreading of the rise times of the OD of the different pixels was kept as small as possible, see Fig. 8. In addition the impact of spatial fluctuations was eliminated by normalizing separately each curve between average limiting values assigned to the high-spin fractions 1 and 0 (for determining these limiting values, a preliminary fit of the selected curve by a *tanh*-law was performed). As a result of these separate normalizations, the overall fluctuations in the HS and LS states were comparable and the overall signal/noise ratio was small, see Fig. 8. The data were analyzed in the frame of the nucleation and growth processes. In a first step we fitted the normalized kinetic curves to a KJMA-type law,[33]

$$\mathrm{OD(t)} \propto 1 - \exp[-\mathrm{k(t-t_0)}]^{\mathrm{n}}. \qquad (1)$$

We obtained exponent values sizably scattered in the range $\sim$[0.2–1.0]. Average parameter values are $n = 0.55$ (0.25) and $k \sim 1.5\ \mathrm{s}^{-1}$. For reducing the scatter of the data we determined an average kinetic curve by summing up the separate kinetic curves. The resulting average curve, see Fig. 9, also led to an excellent agreement with the KJMA-type law, with $n =$ 0.58 (0.08) and $k = 0.44$ (0.08) s^{-1}. At this stage we should mention that segment (2) in Fig. 3 had to be carefully located so as to obtain beautiful single-step kinetic curves. For some other locations of line (2), the kinetic curves exhibited large oscillations (mirage effect) and/or a stepped character, which suggested that the transformation did not proceed uniformly along the *a*-axis of the crystal. We indeed observed such nonuniform transformations along the stacking axis of the similar 2D polymeric spin-crossover compound Fe-bbtr.[19] As for crystal B we also observed more or less stepped kinetic curves, and for the best single-step ones we obtained $n = 0.67$ (0.05) and $k = 0.52$ (0.03) s^{-1} via an average curve.

II. DISCUSSION

The observation that the local kinetics obeys a nucleation and growth (NG) process implies the presence of like-spin domains (LSD) smaller than the pixel resolution ($\sim$2.5 μm). This is consistent with a previous work aiming to resolve LSD patterns by micro-Raman technique,[34] which concluded LSD—if any—should be submicrometric in size. Optical microscopy only monitors the propagation of the conditions suitable for the NG process, which obviously are governed by the propagation of mechanical stresses generated by the volume change. This schematic view is shown as an inset in Fig. 8. In other words the transformation of the crystal is a stress-driven multi-scale process: the low values of the Avrami (KJMA) exponent, here reported, characterize a local process driven by planar diffusion.[35] The suggested existence of planar germs of nucleation is consistent with the 2D polymeric structure of the material, which implies strong intraplane interactions between the spin-crossover molecular units. It is also worth noting that crystals A, B led to close values of the kinetic rate constant k (0.44, 0.52 s^{-1}), despite their very different propagation velocities (2.3, $\sim$10 μm/s, respectively). This observation supports the multiscale character of the process, involving local NG and large-scale propagation, which are governed by different parameters and may occur in rather independent ways.

It should be noted here that the basic assumption of the KJMA theory is simple: negligibly small "droplets" of the equilibrium phase are created inside the uniform metastable phase and subsequently grow without substantial deformation. The growing droplet is also assumed to be randomly placed and overlap freely, with the result that the remaining volume fraction occupied by the metastable phase decays exponentially with the power time law given in Eq. (1). Both the rate constant k and the "Avrami exponent" depend on the spatial dimension and on the details of the nucleation and growth process.

It is worth comparing the present (local) values of the KJMA parameters to those (large scale) obtained by x-ray investigation,[6] $n \sim 2.2$ (1) and $k \sim 0.0069$ (1) s^{-1}, which are to be associated with the average behavior of the crystal. We show in Fig. 9 the superposition of the local kinetic curves recorded on the different pixels of line (1), which cross the entire crystal leading to the fitted KJMA parameters $n = 1.40$ (0.08) and $k = 0.029$ (0.0001) s^{-1}, which indeed are closer to the x-ray values. The marked difference between the local and the macroscopic parameter values again illustrates the multiscale character of the process.

It is worth pointing out that the multiscale character of the process presently seems to be out of reach for the current theoretical works. Simulations reported so far[36–39] have led to snapshots which basically differ from the present experimental images, with the simultaneous occurrence of nuclei at all corners (or edges) of the lattice. These simulations may provide a correct picture of the nucleation and growth process in a nano-particle but obviously fail to represent the propagation effects that are relevant at the meso- or macroscopic scales.

III. CONCLUSION

The crucial role of optical microscopy for the investigation of first-order phase transitions at the solid state was again illustrated here on the example of SMS. We have followed the spatiotemporal aspects of the thermal transition of $[Fe(btr)_2(NCS)_2]\cdot H_2O$ crystals by optical microscope means.

The data analyzed here refer to the first cooling of a given high-quality crystal. We measured propagation velocities of the transformation fronts in the range ∼1–10 μm/s, and the crucial role of stresses was confirmed. We showed that the kinetics of transformation locally follows a KJMA law, the parameter values of which strongly depart from macroscopic values associated to the average behavior of the crystal, and this way we established the multiscale character of the transformation. Such a work is in line with the KJMA analysis of photo-induced transformations reported for various systems in recent literature.[40–42] Thanks to careful inspection of the images and suitable processing, we characterized optical effects resulting from the impact of mechanical stresses upon the refractive index of the crystal. We also gave a first insight to the spatiotemporal aspects of the transition and their local fluctuations (instant velocities, rise times of the local transformation). The quantitative analysis of the spatiotemporal properties based on real-time imaging of the crystal under transformation, with complete mapping of the local kinetics parameters, is planned.

ACKNOWLEDGMENTS

The authors thank E. Collet and H. Cailleau [IPR Rennes] for scientific assistance; J. C. Ameline, L. Toupet [IPR Rennes], G. Bouchez, and E. Codjovi (Versailles) for technical assistance; CNRS, Versailles, and Rennes Universities, Conseil Régional d'Ile de France (C'Nano, projet COLLE) for financial support; and CEFIPRA for postdoctoral grant of H. Mishra.

*kbo@physique.uvsq.fr

[1] Topics in Current Chemistry 233–235, *Spin Crossover in Transition Metal Compounds I –III*, edited by P. Gütlich and H. A. Goodwin (Springer, Heidelberg, Berlin, 2004).
[2] M. Soraï and S. Seki, J. Phys. Chem. Solids **35**, 555 (1974).
[3] M. Soraï, Chem. Soc. Jpn. **74**, 2223 (2001).
[4] H. Spiering, E. Meissner, H. Köppen, E. W. Müller, and P. Gütlich, Chem. Phys. **68**, 60 (1982).
[5] H. Spiering, T. Kohlhaas, H. Romstedt, A. Hauser, C. Bruns-Yilmaz, J. Kusz, and P. Gütlich, Coord. Chem. Rev. **190–192**, 629 (1999).
[6] S. Pillet, V. Legrand, M. Souhassou, and C. Lecomte, Phys. Rev. B **74**, 140101 (2006).
[7] I. Krivokapic, C. Enachescu, R. Bronisz, and A. Hauser, Inorg. Chim. Acta **361**, 3616 (2008).
[8] Y. V. Mnyukh, *Fundamentals of Solid State Phase Transitions, Ferromagnetism and Ferroelectricity*, 1st Books, ISBN: 0-75960-219-0 (Fairfield, USA, 2001).
[9] F. H. Herbstein, Acta Cryst. B **62**, 341 (2006).
[10] A. I. Kitaigorodskiy, Y. V. Mnyukh, and G. Asadov, J. Phys. Chem. Solids **26**, 463 (1965).
[11] Y. V. Mnyukh and N. N. Petropavlov, J. Phys. Chem. Solids, **33**, 2079 (1972).
[12] G. R. Desiraju, I. C. Paul, and D. Y. Curtin, J. Amer. Chem. Soc. **99**, 1594 (1977).
[13] M. Buron-Le Cointe, M. H. Lemée-Cailleau, H. Cailleau, B. Toudic, A. Moréac, F. Moussa, and C. Ayache, Phys. Rev. B **68**, 064103 (2003).
[14] R. R. Chien, Chi-Shun Tu, V.-H. Schmidt, and F.-T. Wang, J. Phys.: Condens. Matter **18**, 8337 (2006).
[15] A. Jákli and G. Liao, Phys. Rev. E **74**, 041706 (2006).
[16] S. Bonnet, M. A. Siegler, J. S. Costa, G. Molnar, A. Bousseksou, A. L. Spek, P. Gamez, and J. Reedijk, Chem. Commun. 5619, (2008).
[17] S. Bedoui, G. Molnár, S. Bonnet, C. Quintero, H. J. Shepherd, W. Nicolazzi, and A. Bousseksou, Chem. Phys. Lett. **499**, 94 (2010).
[18] C. Chong, *Observations et modélisation d'effets d'auto-organisation dans les solides thermo et photo commutables*, PhD Thesis, University of Versailles (Versailles, France, 2010).
[19] C. Chong, A. Slimani, F. Varret, K. Boukheddaden, E. Collet, J.-C. Ameline, R. Bronisz, and A. Hauser, Chem. Phys. Lett. **504**, 29 (2011).
[20] F. Varret, A. Slimani, K. Boukheddaden, C. Chong, H. Mishra, E. Collet, J. Haasnoot, and S. Pillet, New J. Chem. (in press), doi: 10.1039/c1nj20332k.
[21] J. Jeftic, F. Varret, A. Hauser, O. Roubeau, M. Matsarski, and J.-P. Riviera, J. Mol. Cryst. and Liq. Crystals **335**, 511 (1999).
[22] A. Goujon, F. Varret, K. Boukheddaden, C. Chong, J. Jeftic, Y. Garcia, A. D. Naik, J. C. Ameline, and E. Collet, Inorg. Chim. Acta **361**, 4055 (2008).
[23] C. Chong, H. Mishra, K. Boukheddaden, S. Denise, E. Collet, J.-C. Ameline, A. D. Naik, Y. Garcia, and F. Varret, J. Phys. Chem. B **114**, 1975 (2010).
[24] V. Legrand, S. Pillet, C. Carbonera, M. Souhassou, J.-F. Létard, P. Guionneau, and C. Lecomte, Eur. J. Inorg. Chem. 5693 (2007).
[25] H. Constant-Machado, J. Linarès, F. Varret, J. G. Haasnoot, J. P. Martin, J. Zarembowitch, A. Dworkin, and A. Bousseksou, J. Phys. I France **6**, 1203 (1996).
[26] H. Constant-Machado, A. Stancu, J. Linarès, and F. Varret, IEEE Trans. Mag. **34**, 2213 (1998).
[27] W. Vreugdenhil, J. G. Haasnoot, O. Kahn, P. Thuery, and J. Reedijk, Polyhedron **4**, 1769 (1985).
[28] S. Pillet, J. Hubsch, and C. Lecomte, Eur. Phys. J. B **38**, 541 (2004).
[29] See Supplemental Material at http://link.aps.org/supplemental/10.1103/PhysRevB.84.094442 for video A.
[30] See Supplemental Material at http://link.aps.org/supplemental/10.1103/PhysRevB.84.094442 for video B.
[31] J. Y. Jo, S. M. Yang, T. H. Kim, H. N. Lee, J.-G. Yoon, S. Park, Y. Jo, M. H. Jung, and T. H. Noh, Phys. Rev. Lett. **102**, 045701 (2009).
[32] See Supplemental Material at http://link.aps.org/supplemental/10.1103/PhysRevB.84.094442 for video C.
[33] M. Avrami, J. Chem. Phys. **7**, 1103 (1939).
[34] G. Molnar, A. Bousseksou, A. Zwick, and J. G. McGarvey, Chem. Phys. Lett. **367**, 593 (2003).
[35] J. W. Christian, *The theory of transformation of metals and alloys*, (Pergamon Press, Oxford, 1975), pp. 525–548.

[36]M. Nishino, K. Boukheddaden, Y. Konishi, and S. Miyashita, Phys. Rev. Lett. **98**, 247203 (2007).
[37]C. Enachescu, L. Stoleriu, A. Stancu, and A. Hauser, Phys. Rev. Lett. **102**, 257204 (2009).
[38]M. Nishino, C. Enachescu, S. Miyashita, K. Boukheddaden, and F. Varret, Phys. Rev. B **82**, 020409(R) (2010).
[39]C. Chong, F. Varret, and K. Boukheddaden, Phys. Rev. B **81**, 014104 (2010).
[40]D. Papanikolaou, S. Margadonna, W. Kosaka, S. I. Ohkoshi, M. Brunelli, and K. Prassides, J. Amer. Chem. Soc. **128**, 8358 (2006).
[41]Y. Fukuyama, N. Yasuda, J. Kim, H. Murayama, Y. Tanaka, S. Kimura, K. Kato, S. Kohara, Y. Morimoto, T. Matsunaga, R. Kojima, N. Yamada, H. Tanaka, T. Ohshima, and M. Takata, Appl. Phys. Express **1**, 045001 (2008).
[42]M. Ito, H. Kamioka, and Y. Morimoto, J. Phys. Soc. Jpn. **80**, 02370 (2011).